The Effect of 3-(Glycidoloxy Propyl) Trimethoxy Silane Concentration on Surface modification of SiO_2 nanoparticles

Hamed Bahramnia
Semnan University
Hamidreza Mohammadian Semnani (hmohammadian@semnan.ac.ir)
Semnan university
Ali Habibolahzadeh
Semnan University
Hassan Abdoos
Semnan University

Research Article

Keywords: SiO2 nanoparticles, Surface modification, Silanization, 3-(glycidoloxy propyl) trimethoxy silane, Optimal concentration

Posted Date: April 12th, 2021

DOI: https://doi.org/10.21203/rs.3.rs-381518/v1

Version of Record: A version of this preprint was published at Silicon on July 29th, 2021. See the published version at https://doi.org/10.1007/s12633-021-01237-7.

Abstract

Abstract

Coupling agent concentration plays a key role in functionalization of SiO_2 nanoparticles as reinforcing particles.

Purpose

In this study, the influence of 3-(glycidoloxy propyl) trimethoxy silane (GPTMS) concentration on functionalization of SiO_2 nanoparticles, is experimentally investigated.

Methods

The functionalization of nano-silica were performed by 30, 50, 80 and 110 wt.% of GPTMS in order to find the optimal GPTMS concentration to complete the process. Fourier Transformation Infrared Spectroscopy (FTIR), Field Emission Scanning Electron Microscopy (FESEM), Thermo Gravimetric Analysis (TGA) and X-Ray Diffraction (XRD) characterized the pure and modified samples; then, the results were compared to each other to achieve the aim of the research.

Results

FTIR results confirmed the silanization proceed due to the silane absorption peak disappearing and **shifting of the hydroxyl group bonds in to the amide bonds**. This test showed that 30 wt.% GPTMS has not been sufficient for full functionalization of the NPs. According to FESEM images, it seems that the NPs were better modified by 80 wt.% GPTMS due to the least NPs aggregation and lack of coupling agent deposition on the NPs. Also, TGA illustrates that this sample has higher thermal stability because of lower weight loss (11.2%) in coupling agent decomposition temperature range: 130-380°C. Furthermore, X-Ray Diffraction confirmed the FESEM and TGA results about the mentioned sample due to its highest crystallite size (increase 26.64% in crystallite size in comparison with the pure sample).

Conclusion

So, the 80 wt.% of GPTMS introduced as the optimal concentration for surface modification of SiO_2 nanoparticles.

1. Introduction

Silicon dioxide nanoparticles is known as the first produced nanoparticles (NPs) among inorganic materials [1]. This white powder can be found in two major forms; P-type (Porous particles) and S-type (Spherical particles) according to the NPs structure [2]. P-type nano-silica surface containing a number of nano-porous has much larger Specific Surface Area (SSA) comparing to S-type. They have been widely used in nanocomposite preparation due to their excellent properties [3].

Many researchers have been reported that nano-silica could enhance the mechanical and thermal properties of the polymeric matrix, such as toughness, stiffness[4], tensile strength, elongation [5], heat resistance[6], hardness [7] ,wear resistance [8], adhesion to steel substrate [9] and optical properties [10]. These properties improvements have been mentioned due to hydrogen bonds between nano-silica surface polar groups (-OH) and polar groups of the polymer chains[11]. However, the effects of these NPs on nanocomposites properties, also depends on proper dispersion within the matrix and how to react with the polymer chains [12].

NPs tend to agglomerate in the matrix due to their size and very high surface energy. There are some experiences in prevention of nano-silica agglomeration and increasing of NPs surface reactivity due to surface modification by physical and chemical treatments [13–17]; however, the most common method to modify the nano-silica surfaces is organo-silane chemical treatment which can establish strong chemical bond between the NPs surfaces and polymer chains [4].

Silane structure can be introduced as $(RO)_3$-Si-R'-X which RO, R' and X refers to hydrolysable group, alkylene group and organo functional group, respectively. "RO" and "X" established strong bonds between the NPs and polymer chains, respectively [18]. Amine groups also created strong bonds between the silane compounds and the polymeric matrix [19].

Recently, silanization of nano-silica processes have been reported in many papers; however, except for few of them, the optimal concentration of the required silane compounds for this issue has not been investigated. For instance, Xu and et al. [20] didn't even mention the exact ratio of used silane compounds to surface modification of nano-silica. In other examples, Chuang and et.al. [21] as like as Ghosh and et al. [22] mentioned this ratio but didn't discuss about different silane concentrations effect on this process. Although, Rong et al. [23] have studied the effect of different silane concentrations (from 10 up to 30 wt.%) on nano-silica functionalization and introduced 30 wt.% silane as optimal amount; the effect of using more than 30 wt.% silane in this process has not been investigated.

So, in this study, nano-SiO_2 functionalization was started by using 30 wt.% silane and continued with higher silane concentrations. The proper methods characterized the samples to determine the effect of silane concentration on SiO_2 NPs surface modification.

2. Materials And Experimental Procedures

2.1 Materials

Materials, which were used in the experiments, are introduced in Table 1.

Table 1. Materials specifications

Chemicals						
Material's Name	**Trade mark**	**Chemical Formula**	**Purity**	**Molar Mass [g/mol]**	**Density [g/cm^3]**	**Supplier**
3-(glycidoloxy propyl) trimethoxy silane	GPTMS	$C_9H_{20}O_5Si$	>98%	236.34	1.07	Merck Co.
Ethanol	---	C_2H_5OH	96%	---	0.81	Merck Co.
hydrochloric acid	---	HCl	37%	36.46	1.19	Merck Co.

Nanoparticles					
Name	**Purity**	**Size [nm]**	**SSA* [m^2/g]**	**Molar Mass [g/mol]**	**Supplier**
SiO_2 nanoparticles	99.5	20	210	60.8	Merck Co.

* Specific Surface Area

2.2 Surface modification

1 g of raw nano-silica was added to 30 ml solution of distilled water/ethanol 96% (1:1) and it was stirred to obtain uniform solution. Then, 30, 50, 80 and 110 wt.% (with respect to nano-SiO_2 weight) of GPTMS as coupling agent was added to the solution; and in order to set PH of the solution on 4, 0.01 mol of HCl (37%) was added. Mechanical stirrer (1000 rpm) for 30 min stirred the resulted solution and heilscher ultrasonic homogenizer, UIP1000hd, 20 kHz, 1000 W, Germany, with amplitude of 90% for 5 minutes homogenized it. MSE MISTRAL 3000E, U.K (5000 rpm for 30 min), centrifuged the homogenized solution and the resulted gel was dried in a vacuum oven at 80 °C for 36 hours to complete the silanization process of nano-SiO_2.

2.3 Characterization

The success of functionalization process was examined by FTIR spectroscopy on GPTMS and pure/functionalized nano-silica using BRUKER-VERTEX 70, Germany, in the frequency range of 4000-400 cm^{-1}.

Moreover, Morphology of the specimens were investigated using FESEM, MIRA 3-XMU TESCAN, Czech Republic, SEM HV: 15.0 Kv and MAG: 250 Kx.

Furthermore, Thermo Gravimetric Analysis (TGA) analyzed thermal stability of the functionalized samples (according to ASTM E1131. ISO 11358 standards) in such a way that about 10 mg of each samples were heated from 25 to 800° C in N_2 atmosphere, at rate of 10 K min^{-1}, using METTLER TOLEDO, U.S., instrument.

Finally, XRD method performed phase identification and crystallite size determination for the functionalized samples using Bruker, D8 Advanced, Germany, with Cu-Ka radiation and 35KV accelerating voltage. Crystallite size was calculated by using well-known Scherrer equation: [29]

$$D=k\lambda / \beta\cos\theta \qquad (1)$$

Where D is the crystallite size (nm), k is the Scherrer constant (0.91), k is the X-ray wave length (1.5406 A°), b is the full width and half maximum (FWHM), and h is the Bragg angle.

3. Results And Discussion

3.1 FTIR analysis

FTIR method analyzed the possible reactions between nano-SiO_2 and GPTMS during modification process, which shown in Scheme 1.

Fig 1 shows FTIR spectra of the GPTMS, pure nano-silica and surface modified samples with 30 and 50 wt.% GPTMS, respectively. The main IR absorption peaks of GPTMS were observed at 817 cm^{-1} (aromatic C-H bending), 910 cm^{-1} (silane group), 1070 cm^{-1} (Si-O-Si asymmetric stretching), 1340 cm^{-1} (aromatic C-H stretching), 1469 cm^{-1} (C-CH_2), 1729 cm^{-1} (carbonyl group C=O), 1897 cm^{-1} (CO^{2+} $(NO)_2$), 2840 cm^{-1} (C-H symmetric stretching), 2940 cm^{-1} (C-H asymmetric stretching), 3500 ▯ 3600 cm^{-1} (O-H stretching) [19, 24–29]. Further, major bonds of the pure sample can be observed at 1110 cm^{-1} (symmetric Si-O-Si) and 3419 cm^{-1} (hydrogen bonding between hydroxyl groups) [30, 31]. Moreover, in IR spectra of functionalized SiO_2 NPs; symmetric Si-O-Si, C-CH2, C-CH3 and N-H stretching (amide bonds) occurred at 1110 cm^{-1}, 2877 cm^{-1}, 2935 cm^{-1} and 3426 cm^{-1}, respectively [30, 32–34].

Consequently, proceed in modification process was confirmed by FTIR due to disappearing of silane group absorption peak and also shifting the hydroxyl group bonds in to amide bonds in either modified samples. Moreover, disappearing of the silane group peak in IR spectra of functionalized samples illustrated that all the silane groups were consumed in either sample during functionalization process. Furthermore, intensifying the N-H, C-CH3 and C-CH2 peaks by increasing of silane concentration (from 30 wt.% up to 50 wt.%) at 3425 cm^{-1}, 2935 cm^{-1} and 2877 cm^{-1}, respectively, showed that 30 wt.% silane was not sufficient to complete the surface modification process.

So, the study was followed by performing other tests on the samples which modified with 50 wt.% and more silane concentrations.

3.2 FESEM

Fig 2 shows the morphology of the pure and functionalized nano-silica samples with FESEM micrographs. The histogram of the samples also illustrate in Fig 3. The measured average diameters of the NPs in pure sample (Fig 2-a) was 25.72 nm. Mean NPs diameters in functionalized samples with 50, 80 and 110 wt.% of silane, shown in Fig 2-b, 2-c and 2-d, were 25.29, 25.63 and 26.26 nm, respectively. The decrease in NPs average diameter of the functionalized samples compared to the pure sample may be due to the use of hydrochloric acid in functionalization process [35].

According to Fig 2 and 3, as the silane concentration increases in the functionalization process, the NPs average diameter increases. It might be due to increase in bonds between the NPs and coupling agent or silane deposition on the NPs [23].

According to Fig 2-a, nano-SiO_2 particles agglomerated in some areas due to very high surface energy. As shown in Fig 2-b, NPs modification using 50 wt.% GPTMS, appeared to be insufficient because some aggregations were visible. However, NPs functionalization with 80 wt.% GPTMS (Fig 2-c) should be more effective because of the least visible NPs aggregations. Next, Fig 2-d shows that functionalization of the NPs with 110 wt.% GPTMS led to some deposition on the NPs instead of the surface modification.

3.3 Thermal analysis

Thermo Gravimetric analysis was performed on the samples and the resulted curves illustrates in Fig 4. The curves were described in three separated stages in terms of temperature ranges.

In the first stage, in range 25 and 95°C, there were 0.63, 0.8, 0.7 and 1.16% weight losses in pure, 50, 80 and 110 wt.% GPTMS- SiO_2 nanoparticles, due to evaporation of absorbed water during the modification process. The obtained results showed that the amount of water absorption in the last sample was distinctly different from other samples and this might be due to differences in how silane reacted with nano-silica.

The second stage related to thermal stability of the samples against decomposition of the NPs surfaces' silane groups, in range 130 and 380°C. In this stage, it can be seen 0.3, 11.37, 11.2 and 14.65 weight losses percentage in pure, 50, 80 and 110 wt.% GPTMS-nanosilica, respectively. Lack of functional groups on pure sample surfaces caused negligible weight loss during this stage. Thermal stability in this analysis is directly proportional to bonding strength between coupling agent and NPs. Therefore, in TGA, the higher weight losses percentage, the less bonding strength between silane and samples' surfaces. The third stage corresponded to decomposition of nano-silica structures in range 483.5 and 560 °C.

Consequently, TGA confirmed nano-silica functionalization, because there were at least 11.2% weight loss in the specimens, which related to decomposition of silane compounds from nano-silica surfaces in

range 130, and 380 °C. As a result, 80 wt.% GPTMS-SiO_2 NPs was known as better modified sample due to the least weight loss and more stability of grafted coupling agent on the NPs at related temperature range.

3.4 XRD analysis

Fig 5, shows the XRD patterns of the pure and modified nano-silica samples with different coupling agent concentrations. Tetrahedral arrangement of O atoms around the Si atoms caused two dimensional structure with a local short range ordering in amorphous nano-silica [36]. Therefore, there was not any sharp peak in XRD patterns' and as shown in Fig 5, it can be seen only a broad peak related to quartz in range 20 and 22 degree [37–39].

In case of silanization of nano-silica, the characteristic peak in the XRD patterns tends to crystalline mode due to some changes in the ordering of amorphous structure.

The XRD analysis results summarize in Table 2. According to the analysis results, nano-silica functionalization with different amounts of silane groups caused a little change in the broad peaks position in XRD pattern. Therefore, it would be possible to survey the effectiveness of silane concentration on functionalization process with comparing the XRD patterns.

Table 2. XRD analysis data for pure and modified nano-silica with different silane concentrations

Specimen	Pos. [°2θ.]	d-spacing[Å]	FWHM Left. [°2θ.]	D-crystallite size (nm)
Pure nano-silica	20.792	4.2687	0.062	4.0124
50 wt.% GPTMS/ nano-silica	20.856	4.2558	0.054	4.6073
80 wt.% GPTMS / nano-silica	21.310	4.1661	0.049	5.0812
110 wt.% GPTMS / nano-silica	22.287	3.9856	0.077	3.2388

As shown in Fig 5-a, the broad peak was appeared at 20.792° which was related to pure amorphous nano-silica.

According to Fig 5-b and Table 2, nano-silica modification with 50 wt.% silane didn't make much differences in the broad peak shape and position; however, increasing the crystallite size in this sample

(at about 15%) compared with pure nano-silica, showed progress in modification process.

Fig 5-c shows that increase in silane concentration (up to 80 wt.%) in NPs modification process caused to be more crystalline properties of the peak in such a way that intensifies the height of the peak as well as reduces its width. Further, increase in crystallite size (at about 10.3%) in comparison with sample B, confirmed more modification progress in sample C.

Finally, with respect to Fig 5-d, increase in silane concentration up to 110 wt.% in functionalization process of sample D, increased the width of the peak again; and also, according to Table 2, the least crystallite size was reported for this sample (decreasing the crystallite size at about 19.3 % in comparison with the pure sample). It might be due to precipitate the silane on nano-silica instead of modification and increase in disordering of atomic arrangement in microstructure of sample D.

4. Conclusion

This paper investigated the effect of 3-(glycidoloxy propyl) trimethoxy silane concentration on surface modification of SiO_2 nanoparticles in details. So, the pure and functionalized samples with 30, 50, 80 and 110 wt.% GPTMS, were analyzed by FTIR, FE-SEM, TGA and XRD. FTIR analysis confirmed progress of nano-silica functionalization process with GPTMS due to disappearing of the silane absorption peak in functionalized samples and shifting of the hydroxyl group peak in pure sample spectra in to the amide in modified specimens. According to FE-SEM images, increasing the GPTMS concentration in the samples modification caused increase in mean diameter size of the NPs due to grafted silane on the NPs surface; and it seemed functionalization of nano-silica with 80 wt.% GPTMS led to minimal NPs agglomeration and also lack of silane deposition on the NPs surfaces. Furthermore, TGA indicated that 80 wt.% GPTMS grafted sample has higher thermal stability in coupling agent decomposition range at about 130-380 °C among the samples. Moreover, XRD analysis showed that this sample may be better functionalized in comparison with the other samples due to its higher crystallite size. Finally, 80 wt.% GPTMS is introduced as optimal coupling agent concentration for functionalization of the SiO_2 nanoparticles.

Declarations

Acknowledgment The authors would like acknowledge from Ministry of Science, Research and Technology of Islamic Republic of Iran for supporting this work.

Author contributions Bahramnia H. designed and performed experiments, investigated the results and wrote manuscript draft.

Mohammadian Semnani H. supervised the entire research and supported financially the experiments.

Habibolahzadeh A. conceptualized the research.

Abdoos H. performed data curation, reviewed and edited the manuscript.

Funding: This research did not receive any specific grant from funding agencies in the public, commercial, or not-for-profit sectors.

Data availability Electronic supplementary materials contains FTIR, TGA and XRD original data.

Compliance with Ethical Standards Not applicable.

Conflict of interest Authors declared no conflict of interest.

Consent to participate Not applicable.

Consent for publication Not applicable.

References

1. Zhou S-X, Wu L-M, Sun J, Shen W-D (2003) Effect of nanosilica on the properties of polyester-based polyurethane. J Appl Polym Sci 88:189–193. https://doi.org/10.1002/app.11624
2. Orfali WA (2015) Acoustic Properties of Polyurethane Composition Reinforced with Carbon Nanotubes and Silicon Oxide Nano-powder. Phys Procedia 70:699–702. https://doi.org/10.1016/j.phpro.2015.08.091
3. Mirzapour A, Asadollahi MH, Baghshaei S, Akbari M (2014) Effect of nanosilica on the microstructure, thermal properties and bending strength of nanosilica modified carbon fiber/phenolic nanocomposite. Compos Part A Appl Sci Manuf 63:159–167. https://doi.org/10.1016/j.compositesa.2014.04.009
4. Guo Y, Wang M, Zhang H, et al (2008) The surface modification of nanosilica, preparation of nanosilica/acrylic core-shell composite latex, and its application in toughening PVC matrix. J Appl Polym Sci 107:2671–2680. https://doi.org/10.1002/app.27310
5. Petrovic ZS, Javni I, Waddon A, Banhegyi G (2000) Structure and properties of polyurethane-silica nanocomposites. J Appl Polym Sci 76:133–151. https://doi.org/10.1002/(SICI)1097-4628(20000411)76:2<133::AID-APP3>3.0.CO;2-K
6. Blees MH, Winkelman GB, Balkenende AR, den Toonder JMJ (2000) The effect of friction on scratch adhesion testing: application to a sol–gel coating on polypropylene. Thin Solid Films 359:1–13. https://doi.org/10.1016/S0040-6090(99)00729-4
7. Novak BM (1993) Hybrid Nanocomposite Materials?between inorganic glasses and organic polymers. Adv Mater 5:422–433. https://doi.org/10.1002/adma.19930050603
8. Ching YC, Syamimie N (2013) Effect of Nanosilica Filled Polyurethane Composite Coating on Polypropylene Substrate. J Nanomater 2013:1–8. https://doi.org/10.1155/2013/567908
9. Wang F, Feng L, Ma H, et al (2019) Influence of nano-SiO2 on the bonding strength and wear resistance properties of polyurethane coating. Sci Eng Compos Mater 26:77–83. https://doi.org/10.1515/secm-2018-0078

10. Zhou S, Wu L, Sun J, Shen W (2002) The change of the properties of acrylic-based polyurethane via addition of nano-silica. Prog Org Coatings 45:33–42. https://doi.org/10.1016/S0300-9440(02)00085-1
11. Bahramnia H, Mohammadian Semnani H, Habibolahzadeh A, Abdoos H (2020) Epoxy/polyurethane nanocomposite coatings for anti-erosion/wear applications: A review. J Compos Mater 54:3189–3203. https://doi.org/10.1177/0021998320908299
12. Laruelle G, Parvole J, Francois J, Billon L (2004) Block copolymer grafted-silica particles: a core/double shell hybrid inorganic/organic material. Polymer (Guildf) 45:5013–5020. https://doi.org/10.1016/j.polymer.2004.05.030
13. von Werne T, Patten TE (2001) Atom Transfer Radical Polymerization from Nanoparticles: A Tool for the Preparation of Well-Defined Hybrid Nanostructures and for Understanding the Chemistry of Controlled/“Living” Radical Polymerizations from Surfaces. J Am Chem Soc 123:7497–7505. https://doi.org/10.1021/ja010235q
14. Hsiue G-H, Kuo W-J, Huang Y-P, Jeng R-J (2000) Microstructural and morphological characteristics of PS–SiO2 nanocomposites. Polymer (Guildf) 41:2813–2825. https://doi.org/10.1016/S0032-3861(99)00478-4
15. Bialk M, Prucker O, Rühe J (2002) Grafting of polymers to solid surfaces by using immobilized methacrylates. Colloids Surfaces A Physicochem Eng Asp 198–200:543–549. https://doi.org/10.1016/S0927-7757(01)00958-X
16. Yoshinaga K, Shimada J, Nishida H, Komatsu M (1999) Effects of Secondary Polymer Covalently Attached to Monodisperse, Poly(maleic anhydride–styrene)-Modified Colloidal Silica on Dispersibility in Organic Solvent. J Colloid Interface Sci 214:180–188. https://doi.org/10.1006/jcis.1999.6182
17. Wang Q, Xia H, Zhang C (2001) Preparation of polymer/inorganic nanoparticles composites through ultrasonic irradiation. J Appl Polym Sci 80:1478–1488. https://doi.org/10.1002/app.1239
18. Kumudinie C (2001) Polymer–Ceramic Nanocomposites: Interfacial Bonding Agents. In: Encyclopedia of Materials: Science and Technology, Second. Elsevier, pp 7574–7577
19. Bahramnia H, Mohammadian Semnani H, Habibolahzadeh A, et al (2021) The effect of 3-(triethoxy silyl) propyl amine concentration on surface modification of multiwall carbon nanotubes. Fullerenes, Nanotub Carbon Nanostructures 29:74–82. https://doi.org/10.1080/1536383X.2020.1813719
20. Xu MH, Cao YY, Gao SG (2014) Surface Modification of Nano-Silica with Silane Coupling Agent. Key Eng Mater 636:23–27. https://doi.org/10.4028/www.scientific.net/KEM.636.23
21. Chuang W, Geng-sheng J, Lei P, et al (2018) Influences of surface modification of nano-silica by silane coupling agents on the thermal and frictional properties of cyanate ester resin. Results Phys 9:886–896. https://doi.org/10.1016/j.rinp.2018.03.056
22. Ghosh S, Goswami SK, Mathias LJ (2013) Surface modification of nano-silica with amides and imides for use in polyester nanocomposites. J Mater Chem A 1:6073. https://doi.org/10.1039/c3ta10381a

23. Rong Z, Zhao M, Wang Y (2020) Effects of Modified Nano-SiO2 Particles on Properties of High-Performance Cement-Based Composites. Materials (Basel) 13:646. https://doi.org/10.3390/ma13030646
24. Marrone M, Montanari T, Busca G, et al (2004) A Fourier Transform Infrared (FTIR) Study of the Reaction of Triethoxysilane (TES) and Bis[3-triethoxysilylpropyl]tetrasulfane (TESPT) with the Surface of Amorphous Silica. J Phys Chem B 108:3563–3572. https://doi.org/10.1021/jp036148x
25. Derchi G, Manca E, Shayganpour A, et al (2015) Combined Characterization of the Time Response of Impression Materials via Traditional and FTIR Measurements. Materials (Basel) 8:2387–2399. https://doi.org/10.3390/ma8052387
26. Oliveira RN, Mancini MC, Oliveira FCS de, et al (2016) FTIR analysis and quantification of phenols and flavonoids of five commercially available plants extracts used in wound healing. Matéria (Rio Janeiro) 21:767–779. https://doi.org/10.1590/S1517-707620160003.0072
27. Jung MR, Horgen FD, Orski S V., et al (2018) Validation of ATR FT-IR to identify polymers of plastic marine debris, including those ingested by marine organisms. Mar Pollut Bull 127:704–716. https://doi.org/10.1016/j.marpolbul.2017.12.061
28. Robaina NF, de Paula CER, Brum DM, et al (2013) Novel approach for the determination of azithromycin in pharmaceutical formulations by Fourier transform infrared spectroscopy in film-through transmission mode. Microchem J 110:301–307. https://doi.org/10.1016/j.microc.2013.04.015
29. Turnes Palomino G, Otero Areán C, Geobaldo F, et al (1997) FTIR study of CO adsorbed at low temperature on zeolite L Evidence for an ordered distribution of aluminium atoms. J Chem Soc Faraday Trans 93:189–191. https://doi.org/10.1039/a605523k
30. Shahrokh Abadi MH, Delbari A, Fakoor Z, Baedi J (2015) Effects of Annealing Temperature on Infrared Spectra of SiO2 Extracted From Rice Husk. J Ceram Sci Technol 06:41–46. https://doi.org/10.4416/JCST2014-00028
31. Yang W-G, Ha J-H, Kim S-G, Chae W-S (2016) Spectroscopic determination of alkyl resorcinol concentration in hydroxyapatite composite. J Anal Sci Technol 7:9. https://doi.org/10.1186/s40543-016-0089-2
32. Sanches NB, Cassu SN, Dutra R de CL (2015) TG/FT-IR characterization of additives typically employed in EPDM formulations. Polímeros 25:247–255. https://doi.org/10.1590/0104-1428.1819
33. Nandiyanto ABD, Oktiani R, Ragadhita R (2019) How to Read and Interpret FTIR Spectroscope of Organic Material. Indones J Sci Technol 4:97. https://doi.org/10.17509/ijost.v4i1.15806
34. Sayed M, Kamal El-Dean AM, Ahmed M, Hassanien R (2019) Design, synthesis, and characterization of novel pyrimidines bearing indole as antimicrobial agents. J Chinese Chem Soc 66:218–225. https://doi.org/10.1002/jccs.201800115
35. Zhang H, Chen B, Banfield JF (2010) Particle Size and pH Effects on Nanoparticle Dissolution. J Phys Chem C 114:14876–14884. https://doi.org/10.1021/jp1060842

36. Biswas RK, Khan P, Mukherjee S, et al (2018) Study of short range structure of amorphous Silica from PDF using Ag radiation in laboratory XRD system, RAMAN and NEXAFS. J Non Cryst Solids 488:1–9. https://doi.org/10.1016/j.jnoncrysol.2018.02.037
37. Qiu F, Xu H, Wang Y, et al (2012) Preparation, characterization and properties of UV-curable waterborne polyurethane acrylate/SiO2 coating. J Coatings Technol Res 9:503–514. https://doi.org/10.1007/s11998-012-9397-7
38. Wu D, Qiu F, Xu H, et al (2011) Preparation, characterization, and properties of environmentally friendly waterborne poly(urethane acrylate)/silica hybrids. J Appl Polym Sci 119:1683–1695. https://doi.org/10.1002/app.32846
39. de Ferri L, Lottici PP, Lorenzi A, et al (2011) Study of silica nanoparticles – polysiloxane hydrophobic treatments for stone-based monument protection. J Cult Herit 12:356–363. https://doi.org/10.1016/j.culher.2011.02.006

Figures

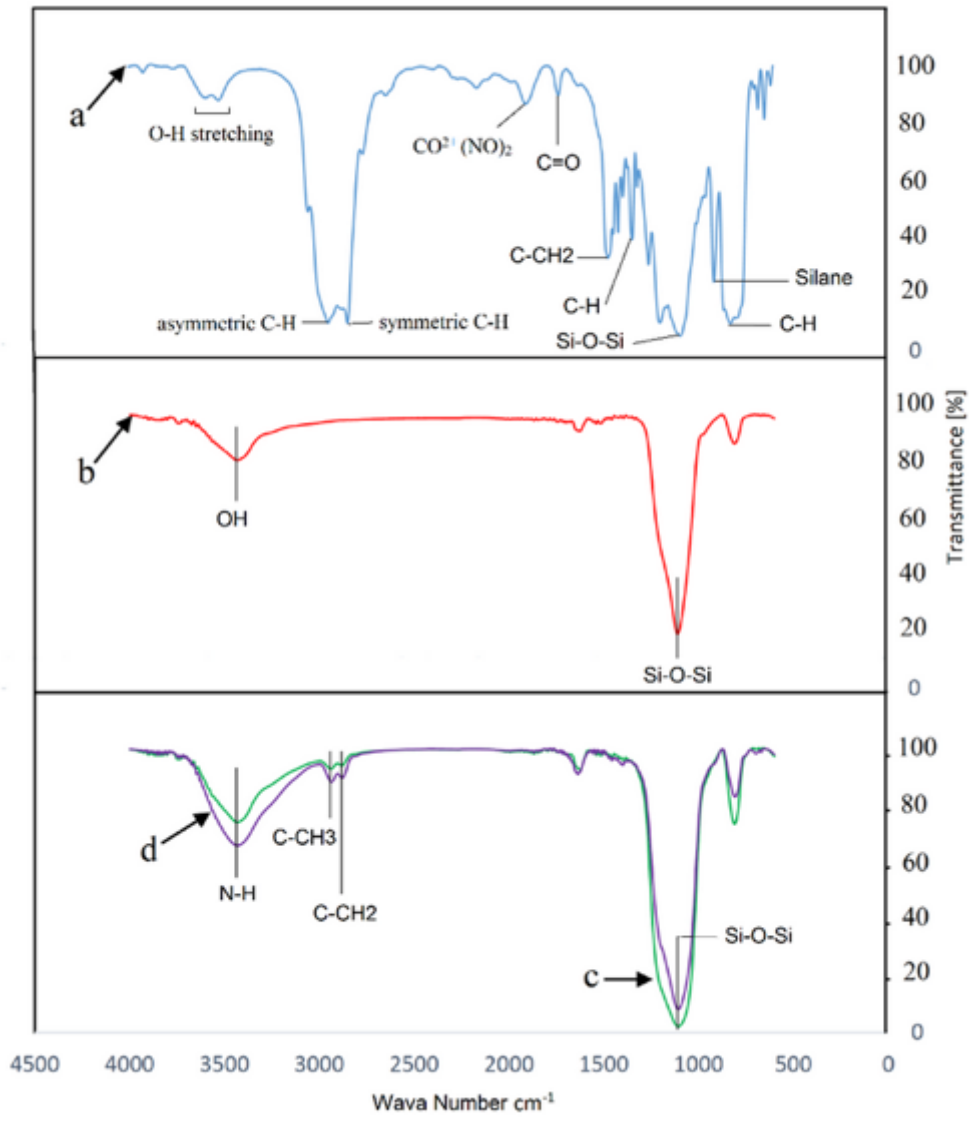

Figure 1

FTIR spectra of (a) GPTMS, (b) pure nano-silica, (c) and (d) surface modified sample with 30 and 50 wt.% GPTMS, respectively

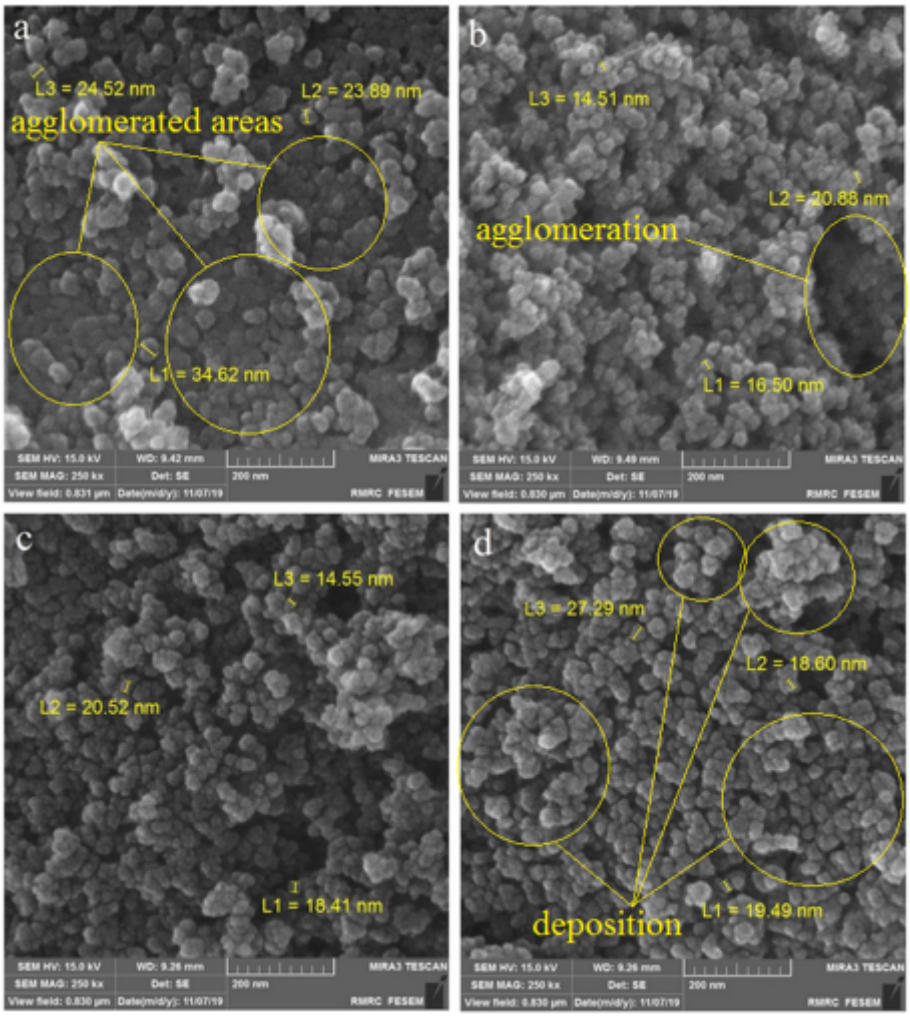

Figure 2

FESEM images of (a) pure sample, (b), (c) and (d) samples modified with 50, 80 and 110 wt.% GPTMS concentrations, respectively

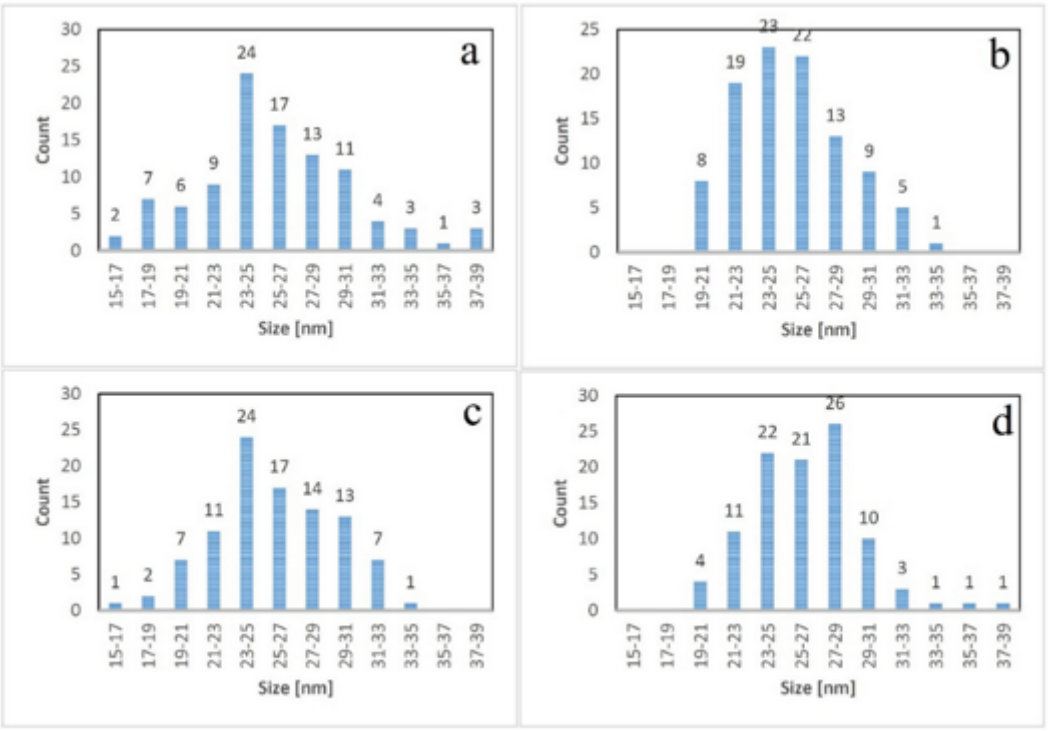

Figure 3

Histogram of (a) pure sample, (b), (c) and (d) samples modified with 50, 80 and 110 wt.% GPTMS concentrations, respectively

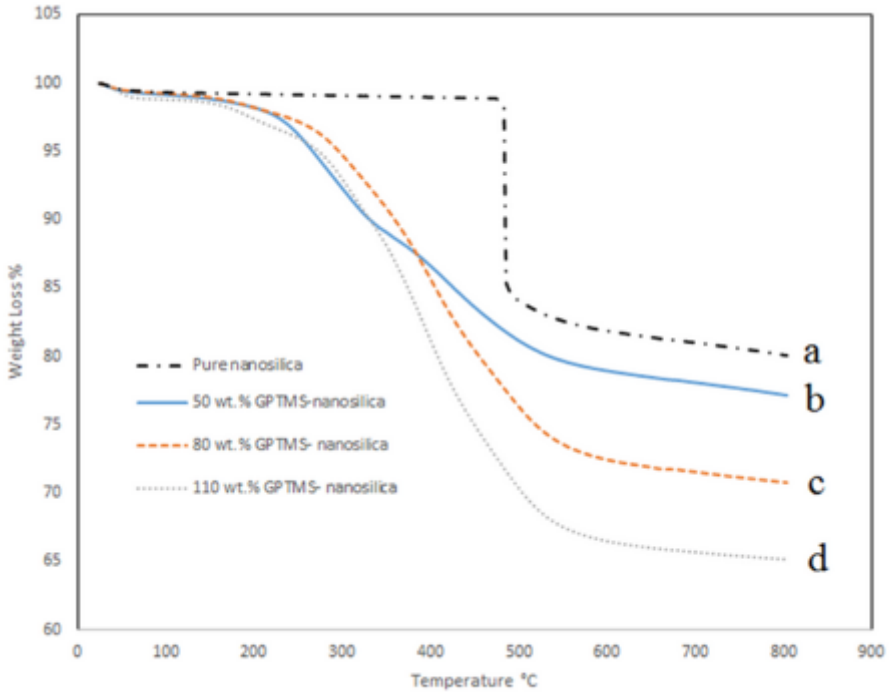

Figure 4

TGA graphs of (a) pure sample, (b), (c) and (d) samples modified with 50, 80 and 110 wt.% GPTMS concentrations, respectively

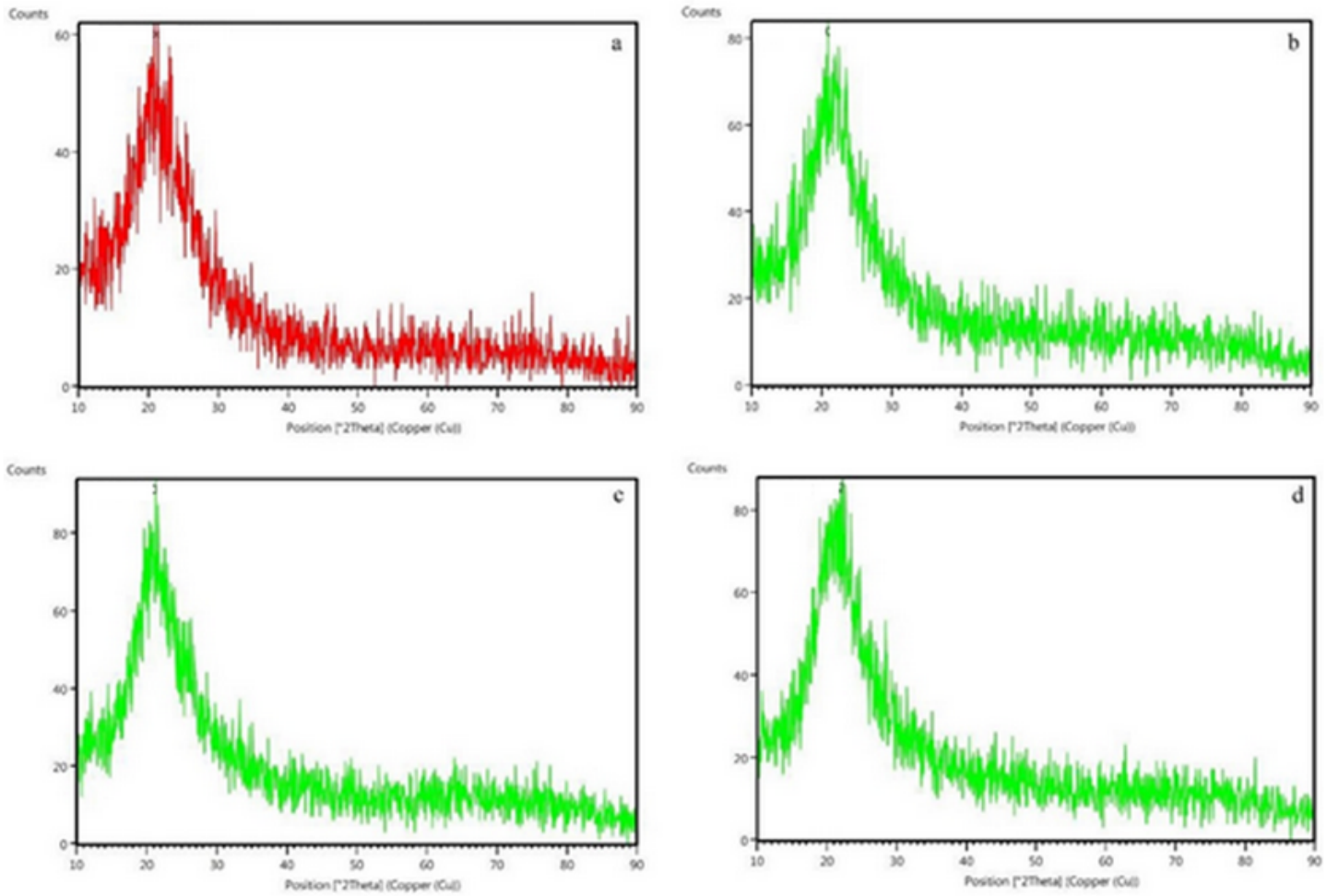

Figure 5

XRD graphs of (a) pure sample, (b), (c) and (d) samples modified with 50, 80 and 110 wt.% GPTMS concentrations, respectively

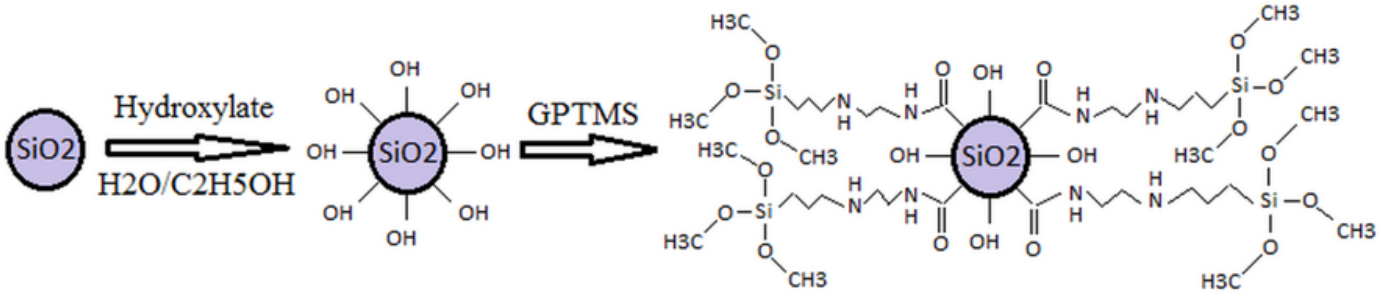

Figure 6

Scheme 1. Nano-SiO2 silanization mechanism

Supplementary Files

This is a list of supplementary files associated with this preprint. Click to download.

- graphicalabstract.tif